

## PROTECTIVE AND FUNCTIONAL POWDER COATINGS

### FORMATION OF PHASES IN THE FePt/Au/FePt FILMS AND THEIR MAGNETIC PROPERTIES

P.V. Makushko,<sup>1,3</sup> M.Yu. Verbytska,<sup>1</sup> M.N. Shamis,<sup>1</sup> A.P. Burmak,<sup>1</sup> Ya.A. Berezniak,<sup>2</sup>  
K.A. Graivoronska,<sup>2</sup> T.I. Verbytska,<sup>1</sup> and Yu.N. Makogon<sup>1</sup>

UDC 539.215.2:661.685

*The effect of annealing atmosphere (vacuum, hydrogen) and intermediate Au layer thickness on the formation of a magnetically hard  $L1_0$  phase and the magnetic properties of  $Fe_{50}Pt_{50}(15\text{ nm})/Au(7.5, 30\text{ nm})/Fe_{50}Pt_{50}(15\text{ nm})$  films deposited by magnetron sputtering onto  $SiO_2(100\text{ nm})/Si(001)$  substrates was studied. Samples were heat-treated in a hydrogen atmosphere at 100 kPa. The disordered  $A1$ -FePt phase formed in the as-deposited films. The ordered  $L1_0$ -FePt phase appeared in the film with an intermediate Au (7.5 nm) layer during vacuum annealing at 650 °C. Increase in the intermediate Au layer thickness to 30 nm reduces the ordering temperature to 600 °C. This is promoted by higher compressive stresses in the as-deposited  $Fe_{50}Pt_{50}$  layers with a thicker Au interlayer. In hydrogen annealing, the  $A1 \rightarrow L1_0$ -FePt phase transition in the  $Fe_{50}Pt_{50}(15\text{ nm})/Au(7.5, 30\text{ nm})/Fe_{50}Pt_{50}(15\text{ nm})$  films starts at 500 °C regardless of the intermediate Au layer thickness. The Au and FePt axial (111) textures are observed in the films annealed in hydrogen. This is more evident in the films with a thicker Au (30 nm) interlayer. The film with an intermediate Au (30 nm) layer shows 27.3 kOe coercivity after vacuum annealing at 900 °C. The same coercivity can be achieved by hydrogen annealing at 700 °C, which is 200 °C lower than after vacuum annealing due to the introduction of hydrogen into voids of the  $L1_0$ -FePt lattice and increase of stresses.*

**Keywords:** film, ordered  $L1_0$ -FePt phase, hydrogen annealing, coercivity.

#### INTRODUCTION

Films produced from the  $Fe_{50}Pt_{50}$  alloy with an ordered  $L1_0$  phase are among promising materials for high-density magnetic recording. These materials show high magnetocrystalline anisotropy energy ( $K_u = 7 \cdot 10^6\text{ J/m}^3$ ) and thermal stability of grains up to 2.8–3.3 nm in size. The recorded data can remain stable over a decade [1–6].

A disordered  $A1$ -FePt phase with magnetically soft properties emerges in the as-deposited films. Heat treatment is required to form a chemically ordered  $L1_0$ -FePt phase. However, high-temperature annealing leads to

<sup>1</sup>National Technical University of Ukraine ‘Igor Sikorsky Kyiv Polytechnic institute’, Kyiv, Ukraine.

<sup>2</sup>Frantsevich Institute for Problems of Materials Science, National Academy of Sciences of Ukraine, Kyiv, Ukraine.

<sup>3</sup>To whom correspondence should be addressed; e-mail: makushko@outlook.com.

---

Translated from Poroshkova Metallurgiya, Vol. 58, Nos. 3–4 (526), pp. 95–103, 2019. Original article submitted September 10, 2018.

unwanted grain growth. Therefore, the ordering temperature of FePt films needs to be decreased and their magnetic properties need to be improved [5–7].

The use of Au, Ag, or Cu with low surface energy as additional layers can accelerate the ordering process through change in the stress state of the FePt layer and decrease the temperature at which the  $L1_0$  phase appears [5–12]. Internal stresses in the films depend on the additional layer thickness, annealing atmosphere, and heating and cooling rate in the annealing process [13–26].

The annealing atmosphere significantly influences the ordering process. The papers [27, 28] showed that oxygen complicated the mutual diffusion of Fe and Pt layers during annealing in inert gases and vacuum. Contrastingly, the penetration of hydrogen atoms into the crystalline lattice decreases the temperature at which the ordered  $L1_0$ -FePt phase forms [29–31].

Annealing in a hydrogen atmosphere accelerates the  $A1 \rightarrow L1_0$  ordering in AuCu nanoparticles by 100 times compared to vacuum annealing [30].

The objective of this research effort is to examine how the annealing atmosphere (vacuum, hydrogen) and the thickness of intermediate Au layer influence the formation of the magnetically hard  $L1_0$  phase and magnetic properties in  $\text{Fe}_{50}\text{Pt}_{50}(15 \text{ nm})/\text{Au}(7.5, 30 \text{ nm})/\text{Fe}_{50}\text{Pt}_{50}(15 \text{ nm})$  films deposited onto  $\text{SiO}_2$  (100 nm)/Si(001) substrates.

### EXPERIMENTAL PROCEDURE

The nanosized  $\text{Fe}_{50}\text{Pt}_{50}(15 \text{ nm})/\text{Au}(7.5, 30 \text{ nm})/\text{Fe}_{50}\text{Pt}_{50}(15 \text{ nm})$  composite films were produced by magnetron sputtering. The  $\text{Fe}_{50}\text{Pt}_{50}$  (15 nm thick) and Au (7.5 or 30 nm thick) layers were deposited at room temperature onto a single-crystalline Si(001) substrate with a  $\text{SiO}_2$  layer 100 nm thick. Prior to deposition, the chamber was evacuated to  $3 \cdot 10^{-6}$  Pa and the operating Ar deposition pressure was  $3.5 \cdot 10^{-1}$  Pa. The thickness of the deposited layers was measured with a quartz resonator. X-ray reflectometry and Rutherford backscattering methods were also used for this purpose. The error in measuring the film thickness was  $\pm 0.5$  nm.

The samples were annealed in  $\sim 10^{-3}$  Pa vacuum and hydrogen at  $\sim 100$  kPa in a temperature range from 500 to 900°C for 30 sec. The heating rates in vacuum and hydrogen were 5 and 1°C/sec. The film crystalline structure following deposition and annealing was examined by X-ray diffraction employing a BRUKER D8 DISCOVER diffractometer (Cu- $K_\alpha$  radiation source).

The degree to which the  $L1_0$ -FePt phase ordered was evaluated from the  $I(001)/I(002)$  intensity ratio [5, 6, 12]. The orientation of easy magnetization axis  $c$  in direction [001] being perpendicular to the surface was determined from the  $I(001)/I(111)$  intensity ratio. The magnetic properties were evaluated using a SQUID magnetometer (Quantum Design MPMS 3).

The residual stresses in the FePt layer in the film plane were determined by X-ray  $\sin^2(\varphi)$  strain measurement using the (111) FePt reflection by the following equation:

$$\sigma_\varphi = \frac{E}{d_{\psi=0} \cdot (1 + \nu)} \text{tg}\alpha ,$$

where  $E$  is Young's modulus;  $\nu$  is Poisson's ratio;  $d_{\psi=0}$  is interplanar spacing; and  $\text{tg}\alpha$  is slope [13, 28]. Note that the composite films have two FePt layers, each being characterized by different stresses. Hence, we can evaluate only the average strain in the (111) plane.

### RESULTS AND DISCUSSION

X-ray diffraction patterns for the  $\text{Fe}_{50}\text{Pt}_{50}(15 \text{ nm})/\text{Au}(7.5, 30 \text{ nm})/\text{Fe}_{50}\text{Pt}_{50}(15 \text{ nm})$  films after deposition and annealing in vacuum and hydrogen in a temperature range from 500 to 900°C are shown in Fig. 1. The as-deposited films have (111) reflections from the disordered  $A1$ -FePt phase and (111) reflections from Au (Fig. 1a, b).

The ordered  $L1_0$ -FePt phase in the film with an Au intermediate layer 7.5 nm thick emerges (Fig. 1a) during vacuum annealing at 650°C, which is ascertained by the appearance of the superlattice (001) FePt reflection

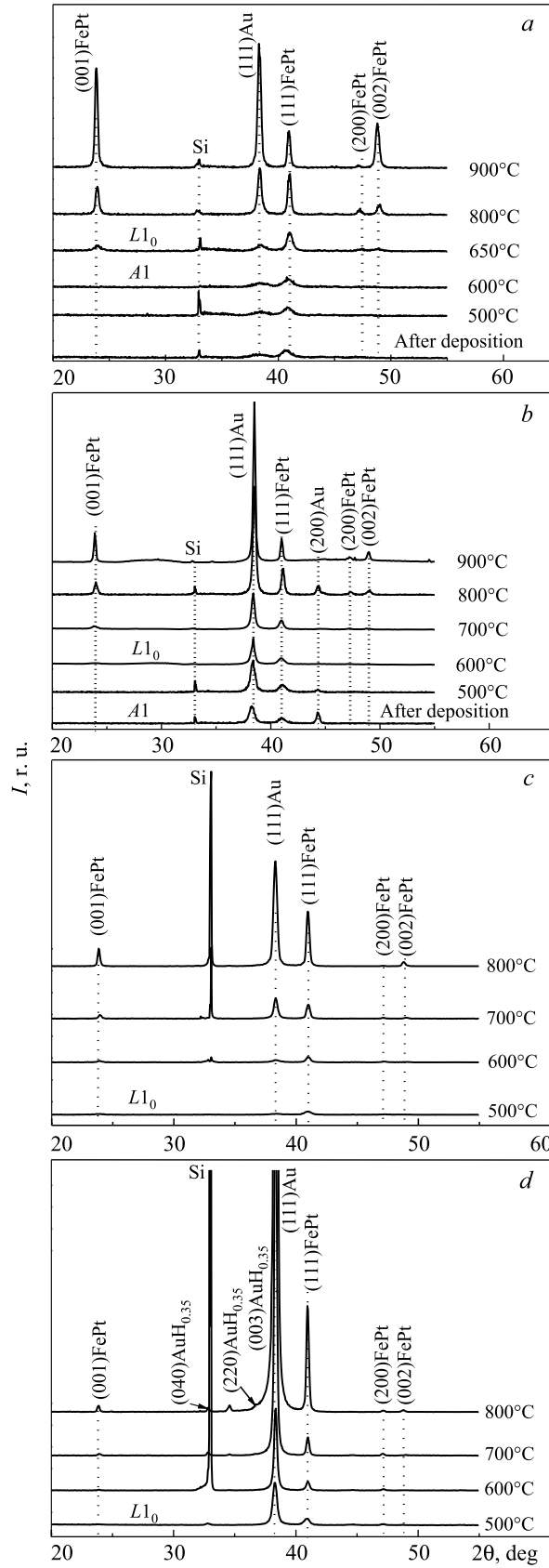


Fig. 1. X-ray diffraction patterns for the Fe<sub>50</sub>Pt<sub>50</sub>(15 nm)/Au(7.5 nm)/Fe<sub>50</sub>Pt<sub>50</sub>(15 nm) (a, c) and Fe<sub>50</sub>Pt<sub>50</sub>(15 nm)/Au(30 nm)/Fe<sub>50</sub>Pt<sub>50</sub>(15 nm) (b, d) films after deposition and annealing in vacuum (a, b) and hydrogen (c, d)

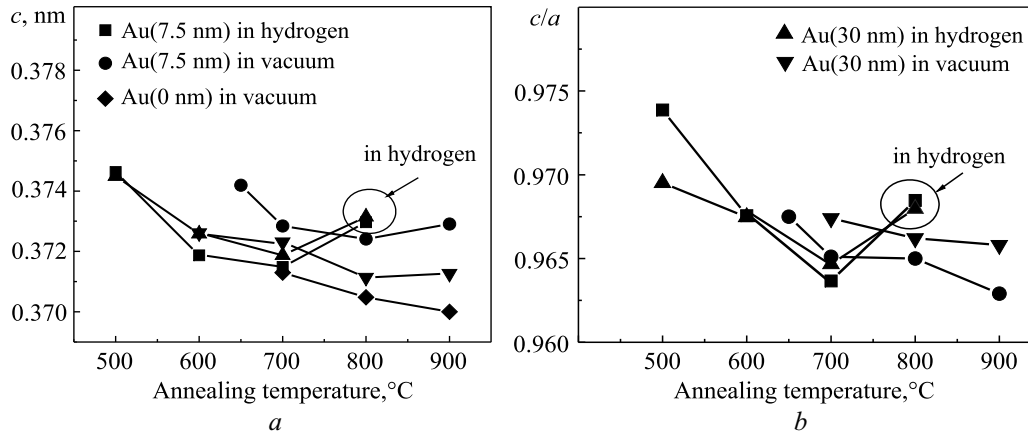


Fig. 2. Dependences of parameter  $c$  (a) and  $c/a$  ratio (b) of the FePt phase on vacuum and hydrogen annealing temperature for the  $\text{Fe}_{50}\text{Pt}_{50}(15 \text{ nm})/\text{Au}(7.5, 30 \text{ nm})/\text{Fe}_{50}\text{Pt}_{50}(15 \text{ nm})$  films

and the splitting of the (200) FePt reflection into (200) and (002). At the same time, the (111) reflection shifts toward higher angles (Fig. 1a).

When the Au layer thickness increases to 30 nm, the ordering temperature decreases to 600°C because of higher compressive stresses in the  $\text{Fe}_{50}\text{Pt}_{50}$  layers after deposition (Fig. 1b). The as-deposited films with an intermediate Au layer 7.5 and 30 nm thick are characterized by the following mechanical stresses in the  $\text{Fe}_{50}\text{Pt}_{50}$  layers:  $-7.5$  and  $-10.5$  GPa.

In vacuum annealing, the ordered  $L1_0$ -FePt phase starts forming in both films at 500°C, which is lower than in vacuum annealing (Fig. 1c, d). This can be attributed to the introduction of hydrogen into voids of the FePt lattice, increase of its parameters, and generation of additional compressive stresses.

Additional reflections appear at angles  $2\theta = 32, 34.5,$  and  $36.7^\circ$  at 600°C (Fig. 1c, d). The intensity of these reflections increases with annealing temperature. We assume that they can belong to  $\text{AuH}_{0.35}$  hydride that results from the introduction of hydrogen atoms into the film. Although  $\text{AuH}_{0.35}$  is unstable at room temperature, this compound was also observed in [32] in nonequilibrium conditions for nanosized films.

The intensity of the (111) Au reflection increases with annealing temperature (Fig. 1). Gold is insoluble in FePt and diffuses along the grain boundaries toward the film surface and film/surface interface. This process enhances the (111) texture of  $L1_0$ -FePt grains, which is more pronounced in films with a thicker Au (30 nm) layer (Fig. 1b). It should be noted that hydrogen annealing leads to more pronounced (111) texture of both Au and FePt (Fig. 1c, d).

The ordering in films annealed in vacuum and hydrogen in a temperature range from 500 to 800°C changes the lattice parameters of the  $L1_0$ -FePt phase. Higher annealing temperature decreases parameter  $c$  and  $c/a$  ratio, being indicative of increase in the tetragonality and ordering of the  $L1_0$ -FePt phase (Fig. 2, Fig. 3a). After hydrogen annealing at 800°C, parameter  $c$  increases and tetragonality decreases (Fig. 2). This is likely to be due to the introduction of hydrogen atoms into octahedral and tetrahedral voids of the crystalline lattice. When vacuum annealing temperature increases to 900°C and intermediate Au layer thickness to 30 nm, the  $L1_0$ -FePt phase becomes more ordered (Fig. 1b, d; Fig. 3a), which is evidenced by greater intensity of the (001) and (002) reflections, resulting from the higher amount of the ordered phase. The  $L1_0$ -FePt grains hardly grow in the [001] direction being perpendicular to the film plane in hydrogen annealing because hydrogen atoms penetrate into the  $L1_0$ -FePt lattice. This is evidenced by lower  $I(001)/I(111)$  ratios compared to vacuum annealing (Fig. 3b).

Our results agree well with the data reported in [30], which showed that oxygen/hydrogen content was important for controlling the crystallographic orientation in the annealing process. The introduction of hydrogen atoms into the film when annealed in a carrier gas (Ar + 3% H) suppresses the growth of grains with easy magnetization axis  $c$  being perpendicular to the film plane.

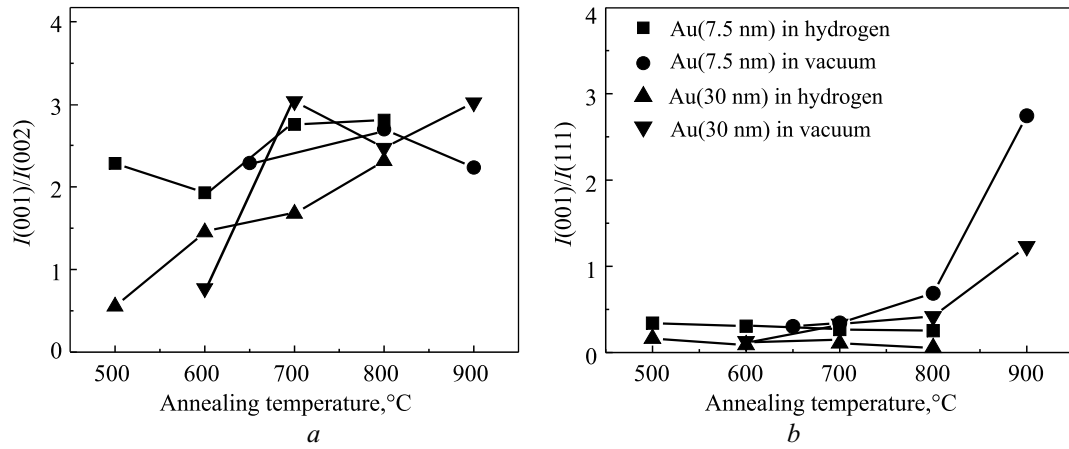


Fig. 3. Dependences of the  $I(001)/I(002)$  (a) and  $I(001)/I(111)$  (b) reflection intensity ratios for the  $L1_0$ -FePt phase in the  $Fe_{50}Pt_{50}(15\text{ nm})/Au(7.5, 30\text{ nm})/Fe_{50}Pt_{50}(15\text{ nm})$  films on annealing temperature

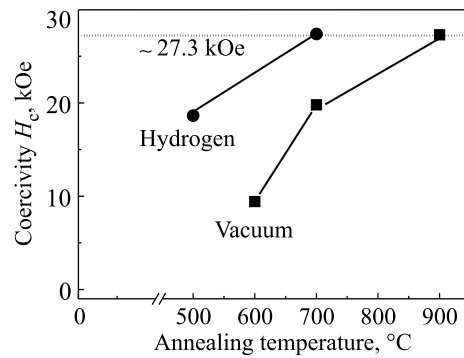


Fig. 4. Dependence of the coercivity in the magnetic field perpendicular to the film plane in films with an intermediate Au (30 nm) layer on vacuum and hydrogen annealing temperature

The structural and phase changes significantly influence the magnetic properties of  $Fe_{50}Pt_{50}(15\text{ nm})/Au(7.5, 30\text{ nm})/Fe_{50}Pt_{50}(15\text{ nm})$  composite films (Fig. 4). Most likely, the diffusion of Au into the FePt layers forms paramagnetic walls along the grain boundaries, thus decreasing the magnetic exchange between them and increasing the coercivity, which becomes higher with thicker walls.

Hydrogen annealing accelerates the ordering process. The introduction of hydrogen atoms into voids of the  $L1_0$ -FePt crystalline lattice and its additional distortions promote higher coercivity. The maximum coercivity (27.3 kOe) in the film with an intermediate Au layer 30 nm thick observed after vacuum annealing at 900°C can be reached by hydrogen annealing at 700°C (Fig. 4).

## CONCLUSIONS

The disordered  $A1$ -FePt phase forms in the film deposition process. The ordered  $L1_0$ -FePt phase appears in the film with an intermediate Au(7.5 nm) layer in vacuum annealing at 650°C.

When thickness of the Au layer increases to 30 nm, the ordering temperature decreases to 600°C because of higher compressive stresses in the as-deposited films. The ordering of the  $L1_0$ -FePt phase becomes greater with annealing temperature being increased to 900°C, which is more pronounced in the films with an intermediate Au layer 30 nm thick.

Regardless of the intermediate Au layer thickness, the ordered  $L1_0$ -FePt phase starts forming in the  $Fe_{50}Pt_{50}(15\text{ nm})/Au(7.5, 30\text{ nm})/Fe_{50}Pt_{50}(15\text{ nm})$  films at lower temperature (500°C) in hydrogen annealing. Predominant (111) Au and FePt textures appear in the process.

Vacuum annealing promotes oriented growth of the  $L1_0$ -FePt grains in the [001] direction.

The ordering process accelerates and the magnetic properties of composite films improve during hydrogen annealing most probably because of higher stresses induced by the introduction of hydrogen into voids of the  $L1_0$ -FePt lattice.

#### ACKNOWLEDGMENTS

The authors would like to thank Professor M. Albrecht and staff of the University of Augsburg (Germany) for preparing the samples, assisting in the research, and discussing the findings. This research effort was funded under the DAAD Leonard Euler Scholar Program (Grant DAAD No. 57198300 and Grant DAAD No. 57291435).

#### REFERENCES

1. D. Weller, A. Moser, L. Folks, M.E. Best, W. Lee, M.F. Toney, M. Schickert, J.-U. Thiele, and M.F. Doemer, "High Ku materials approach to 100 Gbits = in2," *IEEE Trans. Magn.*, **36**, 10–15 (2000).
2. A.T. McCallum, P. Krone, F. Springer, C. Brombacher, M. Albrecht, E. Dobisz, M. Grobis, D. Weller, and O. Hellwig, " $L1_0$  FePt based exchange coupled composite bit patterned films," *Appl. Phys. Lett.*, **98**, 242503 (2011), DOI: 10.1063/1.3599573.
3. D. Weller, O. Mosendz, G. Parker, S. Pisana, and T.S. Santos, " $L1_0$  FePtX–Y media for heat-assisted magnetic recording," *Phys. Status Solidi A*, **210**, 1245 (2013), DOI: 10.1002/pssa.201329106.
4. D. Weller, G. Parker, O. Mosendz, A. Lyberatos, D. Mitin, N.Y. Safonova, and M. Albrecht, "Review article: FePt heat assisted magnetic recording media," *J. Vac. Sci. Technol.*, **B34**, 060801 (2016), DOI: 10.1116/1.4965980.
5. I.A. Vladymyrskyi, O.P. Pavlova, T.I. Verbitska, S.I. Sidorenko, G.L. Katona, D.L. Beke, and Iu.M. Makogon, "Influence of intermediate Ag layer on the structure and magnetic properties of Pt/Ag/Fe thin films," *Vacuum*, **101**, 33 (2014), DOI: 10.1016/j.vacuum.2013.07.018.
6. O.P. Pavlova, T.I. Verbitska, I.A. Vladymyrskyi, S.I. Sidorenko, G.L. Katona, D.L. Beke, G. Beddies, M. Albrecht, and I.M. Makogon, "Structural and magnetic properties of annealed FePt/Ag/FePt thin films," *Appl. Surf. Sci.*, **266**, 100 (2013), DOI: 10.1016/j.apsusc.2012.11.102.
7. T. Maeda, T. Kai, A. Kikitsu, T. Nagase, and J. Akiyama, "Reduction of ordering temperature of a FePt-ordered alloy by addition of Cu," *Appl. Phys. Lett.*, **80**, No. 12, 2147–2149 (2002), DOI: 10.1063/1.1463213.
8. C. Feng, Q. Zhan, B. Li, J. Teng, M. Li, Y. Jiang, and G. Yu, "Magnetic properties and microstructure of FePt/Au multilayers with high perpendicular magnetocrystalline anisotropy," *Appl. Phys. Lett.*, **93**, 152513 (2008), DOI: 10.1063/1.3001801.
9. C. Feng, B.-H. Li, Y. Liu, J. Teng, M.-H. Li, Y. Jiang, and G.-H. Ya, "Improvement of magnetic property of  $L1_0$ -FePt film by FePt/Au multilayer structure," *J. Appl. Phys.*, **103**, 023916 (2008), DOI: 10.1063/1.2828148.
10. Y.S. Yu, H.-B. Li, W.L. Li, M. Liu, and W.D. Fei, "Structure and magnetic properties of magnetron sputtered [(Fe/Pt/Fe)/Au]<sub>n</sub> multilayer films," *J. Magn. Magn. Mater.*, **322**, 1770 (2010), DOI: 10.1016/j.jmmm.2009.12.027.
11. W.Y. Zhang, H. Shima, F. Takano, H. Akinaga, X.Z. Yu, T. Hara, W.Z. Zhang, K. Kimoto, Y. Matsui, and S. Nimori, "Enhancement in ordering of Fe<sub>50</sub>Pt<sub>50</sub> film caused by Cr and Cu additives," *J. Appl. Phys.*, **106**, 033907 (2009), DOI: 10.1063/1.3194313.
12. C.L. Platt, K.W. Wierman, E.B. Svedberg, R. van de Veerdonk, J.K. Howard, A.G. Roy, and D.E. Laughlin, " $L1_0$  ordering and microstructure of FePt thin films with Cu, Ag and Au additive," *J. Appl. Phys.*, **92**, No. 10, 6104–6108 (2002), DOI: 10.1063/1.1516870.
13. Y.F. Ding, J.S. Chen, and E. Liu, "Epitaxial  $L1_0$  FePt films on SrTiO<sub>3</sub>(100) by sputtering," *J. Cryst. Growth*, **276**, 111 (2005), DOI: 10.1016/j.jcrysgro.2004.10.154.
14. M. Albrecht and C. Brombacher, "Rapid thermal annealing of FePt thin films," *Phys. Status Solidi A*, **210**, 1272 (2013), DOI: 10.1002/pssa.201228718.

15. C.L. Zha, S.H. He, B. Ma, Z.Z. Zhang, F.X. Gan, and Q.Y. Jin, "Dependence of ordering kinetics of FePt thin films on different substrates," *IEEE Trans. Magn.*, **44**, No. 11, 3539–3542 (2008), DOI: 10.1109/TMAG.2008.2001609.
16. K.W. Wierman, C.L. Platt, J.K. Howard, and F.E. Spada, "Evolution of stress with  $L1_0$  ordering in FePt and FeCuPt thin films," *J. Appl. Phys.*, **93**, No. 10, 7160–7162 (2003), DOI: 10.1063/1.1555893.
17. S.N. Hsiao, S.K. Chen, T.S. Chin, Y.W. Hsu, H.W. Huang, F.T. Yuan, H.Y. Lee, and W.M. Liao, "Early-stage ordering in in-situ annealed Fe<sub>51</sub>Pt<sub>49</sub> films," *J. Magn. Magn. Mater.*, **321**, 2459–2466 (2009), DOI: 10.1016/j.jmmm.2009.03.018.
18. S.N. Hsiao, F.T. Yuan, H.W. Chang, H.W. Huang, S.K. Chen, and H.Y. Lee, "Effect of initial stress/strain state on order-disorder transformation of FePt thin films," *Appl. Phys. Lett.*, **94**, 232505 (2009), DOI: 10.1063/1.3153513.
19. F.T. Yuan, S.H. Liu, W.M. Liao, S.N. Hsiao, S.K. Chen, and H.Y. Lee, "Ordering transformation of FePt thin films by initial stress/strain control," *IEEE Trans. Magn.*, **48**, No. 3, 1139–1142 (2012), DOI: 10.1109/TMAG.2011.2173660.
20. S.N. Hsiao, S.H. Liu, S.K. Chen, F.T. Yuan, and H.Y. Lee, "Effect of intrinsic tensile stress on (001) orientation in  $L1_0$  FePt thin films on glass substrates," *J. Appl. Phys.*, **111**, 07A702 (2012), DOI: 10.1063/1.3670515.
21. C.H. Lai, C.H. Yang, C.C. Chiang, T. Balaji, and T.K. Tseng, "Dynamic stress-induced low-temperature ordering of FePt," *Appl. Phys. Lett.*, **85**, 4430 (2004), DOI: 10.1063/1.1819985.
22. S.N. Hsiao, S.K. Chen, S.H. Liu, C.J. Liao, F.T. Yuan, and H.Y. Lee, "Effect of annealing process on residual strain/stress behaviors in FePt thin films," *IEEE Trans. Magn.*, **47**, No. 10, 3637–3640 (2011), DOI: 10.1109/TMAG.2011.2147291.
23. S.N. Hsiao, S.H. Liu, S.K. Chen, T.S. Chin, and H.Y. Lee, "Direct evidence for stress-induced (001) anisotropy of rapid-annealed FePt thin films," *Appl. Phys. Lett.*, **100**, 261909 (2012), DOI: 10.1063/1.4730963.
24. J.-S. Kim, Y.-M. Koo, and N. Shin, "The effect of residual strain on (001) texture evolution in FePt thin films," *J. Appl. Phys.*, **100**, 093909 (2006), DOI: 10.1063/1.2364051.
25. J.-S. Kim, Y.-M. Koo, B.-J. Lee, and S.-R. Lee, "The origin of (001) texture evolution in FePt thin films on amorphous substrates," *J. Appl. Phys.*, **99**, 053906 (2006), DOI: 10.1063/1.2176088.
26. W. Hsu, S.K. Chen, W.M. Liao, F.T. Yuan, W.C. Chang, and J.L. Tsai, "Effect of Pt underlayer on the coercivity of FePt sputtered film," *J. Alloys Compd.*, **449**, 52–55 (2008), DOI: 10.1016/j.jallcom.2006.01.113.
27. T. Kamiki and S. Nagawa, "Fabrication of FePt ordered alloy films by annealing in hydrogen atmosphere," *J. Magn. Soc. Jpn.*, **28**, No. 3, 330–334 (2004).
28. T. Kitagawa, J. Ikemoto, T. Kamiki, and S. Nakagawa, "Effect of hydrogen to attain (001) oriented FePt ordered alloy films from Pt/Fe bilayers," in: *IEEE Int. Magn. Conference 2006*, INTERMAG, San Diego, California (2006), pp. 476–476.
29. M. Yamauchi, K. Okubo, T. Tsukuda, K. Kato, M. Takata, and S. Takeda, "Hydrogen-induced structural transformation of AuCu nanoalloys probed by synchrotron X-ray diffraction techniques," *Nanoscale*, **6**, No. 8, 4067–4071 (2014).
30. I.A. Vladymyrskyi, M.V. Karpets, F. Ganss, G.L. Katona, D.L. Beke, S.I. Sidorenko, T. Nagata, T. Nabatame, T. Chikyow, G. Beddies, M. Albrecht, and Iu.M. Makogon, "Influence of the annealing atmosphere on the structural properties of FePt thin films," *J. Appl. Phys.*, **114**, 164314 (2013), DOI: 10.1063/1.4827202.
31. M.Yu. Verbitska, M.N. Shamis, P.V. Makushko, Ya.O. Bereznyak, K.O. Graivoronska, T. I. Verbitska, and Iu.M. Makogon, "Formation of ordered  $L1_0$ -FePt phase in Fe<sub>50</sub>Pt<sub>50</sub>/Au/Fe<sub>50</sub>Pt<sub>50</sub> films in hydrogen annealing," *Metallofiz. Noveish. Tekhnol.*, **40**, No. 8, 1069–1079 (2018).
32. V.E. Antonov, T.E. Antonova, I.T. Belash, A.E. Gorodetskii, and E.G. Ponyatovskii, "Production of gold hydrides at high hydrogen pressure," *Dokl. Akad. Nauk SSSR*, **266**, No. 2, 376–380 (1982).